Supplemental Tables

Table S1. Forelimb vs hindlimb differential expression

Log-linear analysis with LRT-statistic of forelimb and hindlimb RPKMs. Columns are UCSC cluster id, UCSC transcript id, MGI gene symbol, Entrez Gene accession number, forelimb replicate 1 RPKM, forelimb replicate 2 RPKM, hindlimb replicate 1 RPKM, hindlimb replicate 2 RPKM, LRT statistic, raw p-value, Bonferroni corrected p-value, and Benjamani-Hochberg corrected p-value (BHP).

Table S2. DAVID output for FL vs HL differentially expressed genes

Full DAVID output for genes identified as differentially expressed between forelimb and hindlimb in Table S6 (BHP ≤ 0.05).

Table S3. Novel TAR identification and differential expression

Identification and log-linear analysis with LRT-statistic of novel transcriptionally active regions in forelimb and hindlimb. Columns are novel TAR id, chr, start, stop, forelimb replicate 1 RPKM, forelimb replicate 2 RPKM, hindlimb replicate 1 RPKM, hindlimb replicate 2 RPKM, Log_2 fold change, LRT statistic, raw p-value, Bonferroni corrected p-value, and Benjamani-Hochberg corrected p-value (BHP). Coordinates are in BED format (mm9).

Table S4. Novel splice identification

Identification and number of reads supporting each novel splice in each forelimb or hindlimb RNA-seq replicate. Columns are UCSC transcript id, MGI gene symbol, Entrez Gene accession number, junction coordinate, Reads mapping to junction from forelimb replicate 1, forelimb replicate 2, hindlimb replicate 1, hindlimb replicate 2, and average reads mapped from all four replicates.

Table S5. Merged E10.5 limb H3K27ac regions

List of mm9 coordinates in BED format of all merged H3K27ac regions identified in combined limb data.

Table S6. Merged E10.5 limb H3K27me3 regions

List of mm9 coordinates in BED format of all merged H3K27me3 regions identified in combined limb data.

Table S7. Merged E11.5 limb H3K27ac regions

List of mm9 coordinates in BED format of all merged H3K27ac regions identified in combined limb data.

Table S8. Forelimb vs hindlimb differential marking of intergenic and intronic E10.5 H3K27ac regions

Log-linear analysis with LRT-statistic for all limb intergenic and intronic H3K27ac regions between forelimb and hindlimb replicates. Columns are region coordinates, reads from forelimb replicate 1, forelimb replicate 2, hindlimb replicate 1, hindlimb replicate 2, LRT-statistic, raw p-value, Bonferroni corrected p-value, and Benjamani-Hochberg corrected p-value (BHP). Coordiantes are in BED format (mm9).

Table S9. Limb vs MES differential expression statistics

Log-linear analysis with LRT-statistic of combined limb RPKMs and MES RPKMs. Columns are UCSC cluster id, UCSC transcript id, MGI gene symbol, Entrez Gene accession number, limb replicate 1 RPKM, limb replicate 2 RPKM, MES replicate 1 RPKM, MES replicate 2 RPKM, MES replicate 3 RPKM, LRT statistic, raw p-value, Bonferroni corrected p-value, and Benjamani-Hochberg corrected p-value (BHP).

Table S10. Limb vs NPC differential expression statistics

Log-linear analysis with LRT-statistic of combined limb RPKMs and MES RPKMs. Columns are UCSC cluster id, UCSC transcript id, MGI gene symbol, Entrez Gene accession number, limb replicate 1 RPKM, limb replicate 2 RPKM, NPC replicate 1 RPKM, NPC replicate 2 RPKM, LRT statistic, raw p-value, Bonferroni corrected p-value, and Benjamani-Hochberg corrected p-value (BHP).

Table S11. Limb specific intergenic and intronic E10.5 and E11.5 H3K27ac regions

Genomic coordinates of limb specific intergenic and intronic H3K27ac regions identified by k-means clustering in Figure 3A and Figure S8. All coordinates are in BED format (mm9).

Table S12. Enrichment of transcription factor binding sites in top 500 E10.5 limb clustered H3K27ac regions.

Total counts for each motif interrogated by FIMO in the top 500 H3K27ac enriched regions based on signal from E10.5 limb, MES, and NPC. For each category columns are JASPAR id, gene symbol, and occurrence count. Randomization of each tissue specific set is described in methods. Columns are JASPAR id, gene symbol, mean counts, standard deviation, top 95% value, and bottom 5% value for each motif from 1000 shuffled sets of 500 sequences based on limb, MES, or NPC sets.

Table S13. DAVID output for transcription factor motifs specifically enriched in top 500 strongest E10.5 limb H3K27ac regions.

Full DAVID output for transcription factors indicated to have motifs enriched only in top 500 limb sequences compared to a background list of all non-redundant vertebrate JASPAR motifs.

Table S14. Forelimb E10.5 versus E11.5 differential marking of intergenic and intronic H3K27ac regions Fisher's Exact Test output for all E10.5 and E11.5 forelimb intergenic and intronic H3K27ac regions. Columns are region coordinates, reads from e10.5 forelimb, reads from E11.5 forelimb, $\log_2$ fold change, directionality of change, raw p-value, Bonferroni corrected p-value, and Benjamani-Hochberg corrected p-value (BHP). Coordinates are in BED format (mm9).

Table S15. Hindlimb E10.5 versus E11.5 differential marking of intergenic and intronic H3K27ac regions Fisher's Exact Test output for all E10.5 and E11.5 hindlimb intergenic and intronic H3K27ac regions. Columns are region coordinates, reads from e10.5 hindlimb, reads from E11.5 hindlimb, $\log_2$ fold change, directionality of change, raw p-value, Bonferroni corrected p-value, and Benjamani-Hochberg corrected p-value (BHP). Coordinates are in BED format (mm9).

Table S16. PCR Primers

Forward and reverse primers used for validation of differential expression, novel tars, novel splices, and ChIP-seq enriched regions.

Table S17. Sequencing statistics

Total number of raw and uniquely aligned reads in millions (M) for each replicate of RNA-seq or ChIP-seq.

Table S18. Novel TAR coding potential.

Blastx output for 580 novel TARs indicated to have coding potential at an E-value $\leq$ 0.1. Only the top hit for each novel TAR is shown.

Table S19. 2 X 2 contingency table for Fisher exact test

		Read count from tissue of type FL (or HL)		
Read count in each gene	Gene g	FL1 X+1,g	HL1 X+2,g	X.,g
	Not Gene g	X+1,. – X+1,g	X+2,. – X+2,j	X.,. – X.,g
		X+1,.	X+2,.	X.,.

Supplemental Figure Legends

Figure S1. RNA-seq reproducibility and differential expression across limb and MES

A. Scatter plots of $\log_2$(RPKM) values from forelimb and hindlimb replicates. Red and green points represent differentially expressed genes between individual replicates. **B.** Hierarchical clustering of all genes differentially expressed (BHP < 0.05) between limb and MES based on $\log_2$(RPKM) values from each tissue replicate.

Figure S2. Validation of differentially expressed genes, novel TARS and novel splices

A. Bar graphs of differential expression measured by QPCR for 20 selected genes identified by RNA-seq. Values are represented as fold enrichment versus the lower expressed tissue determined by ΔΔCt with *Actb* (error bars +/- s.d., n=4). **B.** Agarose gel of QPCR end products confirming the presence of 11 novel TARs identified by RNA-seq in either forelimb or hindlimb tissue (~100 bp product is positive). **C.** Agarose gel of QPCR end products confirming the presence of 12 novel splices identified by RNA-seq in forelimb tissue (~100 bp product is positive). Larger products likely represent annotated splice forms.

Figure S3. ChIP-seq reproducibility

Scatter plots of log2(RPKM) values calculated for all H3K27 enriched regions in any biological replicate. Red and green points represent regions that are differentially marked between biological replicates. Pearson correlations are indicated for each plot (purple).

Figure S4. Validation of regions identified by ChIP-seq

A. Bar graphs of fold enrichment versus input at selected H3K27me3 regions from forelimb or hindlimb ChIPs. **B.** Bar graphs of fold enrichment versus input at the same sites as A for forelimb or hindlimb H3K27ac ChIPs. All values determined by ΔCt of ChIP and input samples (error bars +/1 s.d., n=4).

Figure S5. Association of differentially marked H3K27ac regions and differentially expressed genes between E10.5 forelimb and hindlimb.

Genome-wide distribution of differentially marked H3K27ac regions between E10.5 forelimb and hindlimb compared to genes differentially expressed between forelimb and hindlimb. For each region the nearest gene transcription start site was assigned up to 200 kb away. Error bars represent the 95% confidence interval from 1000 randomized sets of intergenic and intronic sequences. **A.** Association of regions differentially marked in forelimb with forelimb upregulated genes. **B.** Association of regions differentially marked in forelimb with forelimb upregulated genes compared to hindlimb upregulated genes. In each case enrichment is determined relative to random regions. **C.** Association of regions differentially marked in hindlimb with hindlimb

upregulated genes. **D.** Association of regions differentially marked in hindlimb with hindlimb upregulated genes compared to forelimb upregulated genes. In each case enrichment is determined relative to random regions.

Figure S6. H3K27ac enriched region conservation

Aggregration plot of phastCons scores in a 20kb window centered on each limb EP300 site, limb, limb-specific or limb-MES-NPC marked H3K27ac intergenic or intronic regions.

Figure S7. Transcription factor displacement of H3K27ac modified nucleosomes in limb H3K27ac regions. A. E10.5 limb H3K27ac signal density plots normalized for input surrounding limb enriched motifs for transcription factors expressed highly in top 500 limb regions (red) and all 6027 limb regions (orange) versus those that are expressed at low levels (RPKM <1) (dashed blue). E10.5 limb H3K27ac signal in top 500 limb regions at motifs enriched in MES enhancers and expressed highly in MES show strong signal but no displacement (cyan). E10.5 limb H3K27ac signal also shows displacement at 54 transcription factor binding sites that are enriched in all enhancer classes and expressed at an RPKM > 1 in all three states (green). MES H3K27ac signal at the strong motif/high expression sites shows low signal and no nucleosome displacement (grey). **B.** Depletion of H3K27ac signal coincides with the presence of a strong binding site prediction within a larger H3K27ac enriched region.

Figure S8. K-means clustering of H3K27ac signal at E11.5 Limb, MES, and NPC intergenic and intronic regions. K-means clustering of H3K27ac signals (in RPKM) across 54,358 merged regions, using an 8 kb window centered on the midpoint of each region, revealed three tissue-specific classes of H3K27ac enriched regions. Intergenic and intronic H3K27ac regions in E10.5 and E11.5 limb, MES, and NPC were identified and merged as described in the main text.

Figure S9. Association of differentially marked H3K27ac regions and differentially expressed genes between E10.5 and E11.5 forelimb and hindlimb. Genome-wide distribution of differentially marked H3K27ac regions between E10.5 and E11.5 forelimb and hindlimb compared to genes differentially expressed between E10.5 and E11.5 forelimb and hindlimb. For each region the nearest gene transcription start site was assigned (up to 200 kb away). Error

bars represent the 95% confidence interval from 1000 randomized sets of intergenic and intronic sequences. **A.** Association of regions more strongly marked in E10.5 forelimb with E10.5 forelimb upregulated genes. **B.** Association of regions more strongly marked in E10.5 hindlimb with E10.5 hindlimb upregulated genes. **C.** Association of regions more strongly marked in E11.5 forelimb with E11.5 forelimb upregulated genes. **D.** Association of regions more strongly marked in E11.5 hindlimb with E11.5 hindlimb upregulated genes.

Figure S10. Increasing H3K27ac signal correlates with increased enrichment for tissue specific enhancers and EP300 sites. RPKM was calculated based on the number of H3K27ac ChIP-seq reads for all intergenic and intronic E11.5 H3K27ac enriched regions. These regions were ranked by RPKM and divided into quintile bins (bins 1-5) representing lowest to highest RPKM values. **A.** Overlap of tissue specific EP300 sites with E11.5 H3K27ac regions from each bin. **B.** Percentage of total Vista positive limb, Vista positive non-limb, and Vista negative elements that overlap with E11.5 H3K27ac regions from each bin. **C.** Percentage of bases in each bin occupied by tissue specific EP300 binding events. **D.** Fraction of bases in each bin identified as having limb, non-limb or no enhancer activity normalized per 100,000 bases encompassed by the Vista positive limb, Vista positive non-limb, and Vista negative elements. **E.** GREAT binomial p-values for the "Embryonic Limb Morphogenesis" Gene Ontology category for all H3K27ac regions from each bin.

Figure S11. Developmental enhancers display constitutive signatures across multiple tissues.

A. E10.5 limb H3K27ac signal density normalized for input was determined in a 20kb window surrounding the center of tissue specific EP300 sites or random intronic and intergenic regions (black). **B.** E11.5 limb input signal density was determined in a 20kb window surrounding the center of tissue specific EP300 sites or random intronic and intergenic regions (black). **C.** E11.5 limb input signal density was determined in a 20kb window surrounding the center of tissue-specific H3K27ac regions determined in this study or random intronic and intergenic sites (black). **D.** Input signal density from E10.5 limb, MES, and NPC was determined in a 20kb window surrounding the center of MES specific H3K27ac regions. MES input signal density was also determine over the same window at random intronic and intergenic sites (black).

Figure S12. Known enhancers are marked by H3K27ac in tissues where they show no detectable activity. *Top*. H3K27ac signal in E11.5 limb at a known enhancer (hs1325) from the Vista Enhancer Browser annotated as active in the embryonic brain, but not in limb. H3K27ac is significantly enriched at this site in limb. *Bottom*. A representative transgenic embryo stained for LacZ showing the expression pattern for this enhancer.

Supplemental Methods

RNA-seq and ChIP-seq of Limb Tissue

All animals were sacrificed according to approved Yale IACUC protocols. For RNA-seq, forelimb and hindlimb buds were each dissected from two separate litters of six E10.5 murine embryos in cold PBS and placed in RNALater (Qiagen). Total RNA was extracted using the RNEasy Kit (Qiagen) and prepared for sequencing with the Illumina mRNA-seq Sample Prep Kit. Samples were sequenced on an Illumina GA IIx (35 bp single end (SE) reads).

For each ChIP-seq experiment, forelimb and hindlimb buds from ~50 E10.5 or ~20 E11.5 embryos were dissected as above. For each litter, dissected limb buds were briefly homogenized and crosslinked with 1% formaldehyde at room temperature with rotation for 15 minutes. Crosslinking was quenched and tissue was harvested by centrifugation. Pelleted tissue was washed twice with cold PBS, flash frozen and stored at -80°C. Nuclei were extracted by combining tissue pellets from eight litters in six pellet volumes of lysis buffer I (50 mM Tris pH 8.0, 140 mM NaCl, 1 mM EDTA, 10% glycerol, 0.5% NP-40, 0.25% Triton X-100, 1x Roche Complete Protease inhibitor, 5 mM sodium butyrate) and incubating on ice for 15 minutes. Tissue was homogenized with a dounce homogenizer and nuclei were harvested by centrifugation at 2000g for 10 minutes at 4°C. Nuclei were resuspended in five pellet volumes of nuclear lysis buffer (10 mM Tris pH 8.0, 1 mM EDTA, 0.5 mM EGTA, 0.2% SDS, 1x Roche Complete Protease inhibitor, 5 mM sodium butyrate) and incubated on ice for 20 minutes. 300 μL nuclear lysates in 1.5 mL tubes were sonicated using a Misonix S4000 with 431A cup horn (10 second pulses, 10 second rest, 20 minutes total, 2°C maintained by circulating chiller). Following sonication insoluble material was pelleted by centrifugation at 16000g for 10 minutes at 4°C. A small sample of soluble crosslinked chromatin was purified, checked for correct sonication size range and DNA concentration was measured. 50 μg of chromatin was diluted to

450 μL with dilution buffer (16.7 mM Tris pH 8, 167 mM NaCl, 1.2 mM EDTA, 0.01% SDS, 1.1% Triton X-100, 1x Roche Complete Protease inhibitor, 5 mM sodium butyrate) and added to 50 uL of Protein G Dynabeads (Invitrogen) prebound with 10 μg of antibodies H3K27me3 (Millipore 07-449) or H3K27ac (Abcam ab4729). Samples were incubated overnight at 4°C with rotation. Beads were precipitated on magnet stand and washed five times with 1 mL of wash buffer (100 mM Tris pH8.0, 500 mM LiCl, 1% NP-40, 1% deoxycholic acid, 1x Roche Complete protease inhibitor, 5mM sodium butyrate) and once with TE. Immunoprecipiated chromatin was eluted from beads with 50 μL of elution buffer (TE + 1% SDS) at 65°C for 10 minutes. Crosslinks were reversed overnight at 65°C. Chromatin was treated with RNAseA and proteinase K then purified with Qiagen PCR cleanup kit. Concentration of eluted chromatin was measured with PicoGreen (Invitrogen). Chromatin from H3K27me3 experiments was prepared for sequencing using the Illumina ChIP-seq kit. For H3K27ac experiments chromatin was prepared for sequencing using Illumina ChIP-seq kit with the substitution of Illumina multiplexing adapters and indexing primers. H3K27me3 libraries were sequenced on an Illumina GA IIx (75 bp SE reads). H3K27ac multiplexed libraries were sequenced on an Illumina HiSeq (75 bp PE reads).

Scatter plot with Pearson's Correlation Coefficient (r)

To demonstrate reproducibility of two biological replicates in FL and HL, we performed Pearson correlation analysis based on log scale of raw signals at enriched regions for H3K27ac and H3K27me3. First, differentially marked regions in two replicates of each tissue were identified by the Fisher exact test with a similar way as shown in identification of differentially expressed genes for RNA-seq gene expression profiles. To obtain statistical support for the differences between replicates, pair-wise comparison via Fisher exact test is tested under the null hypothesis that there is no significant difference between two individual experiments for active or repressed chromatin domains in each sample. More stringent Bonferroni corrected p-value at α=0.05 is used as a cutoff criterion here to reduce false discovery rates.

Figure S1

A

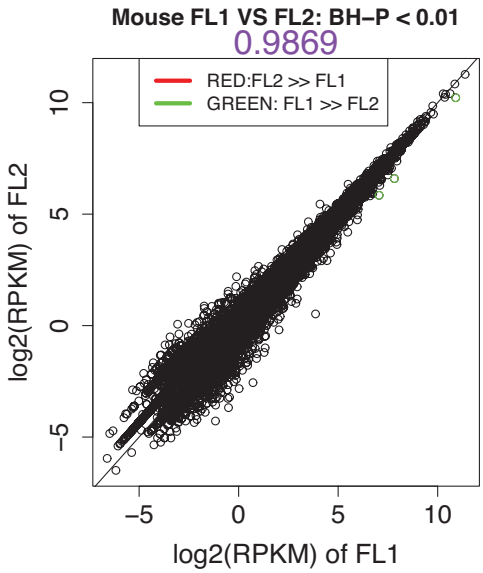

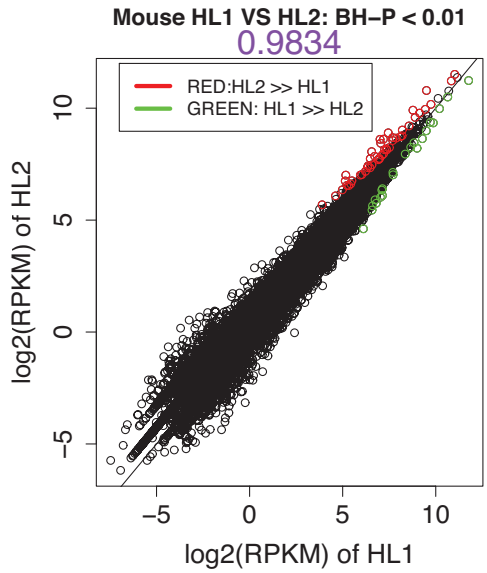

B

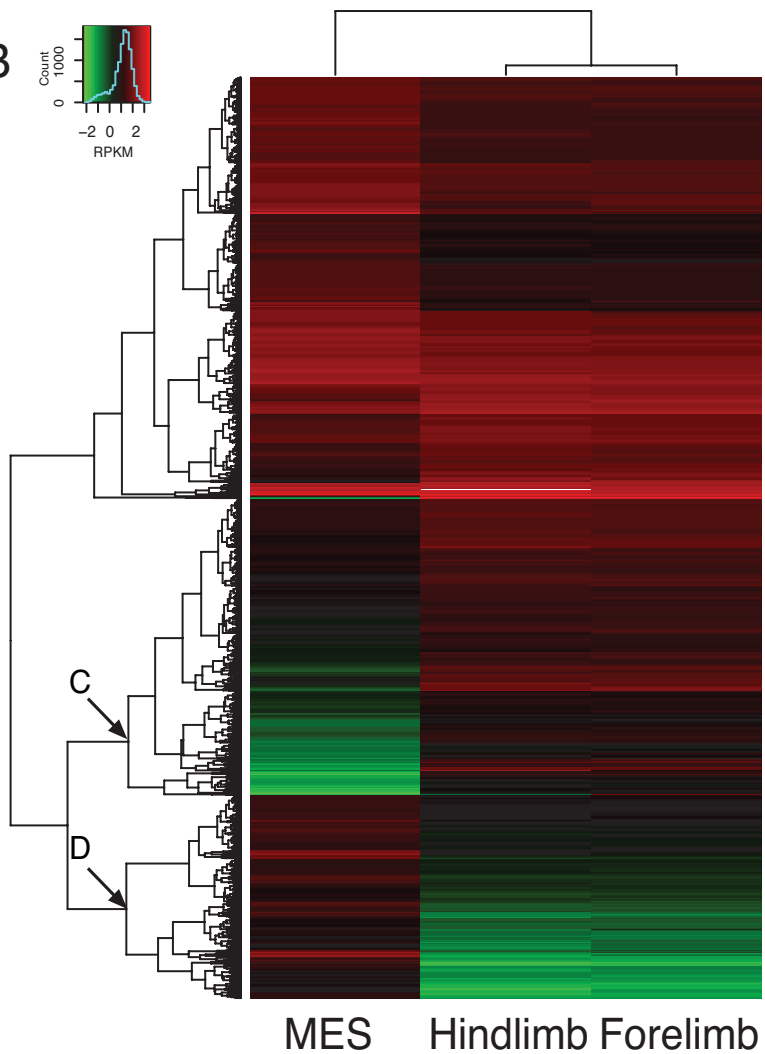

C

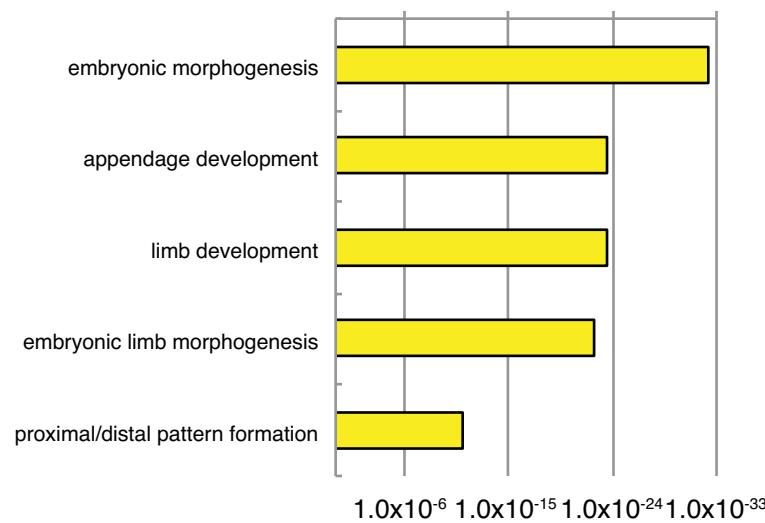

D

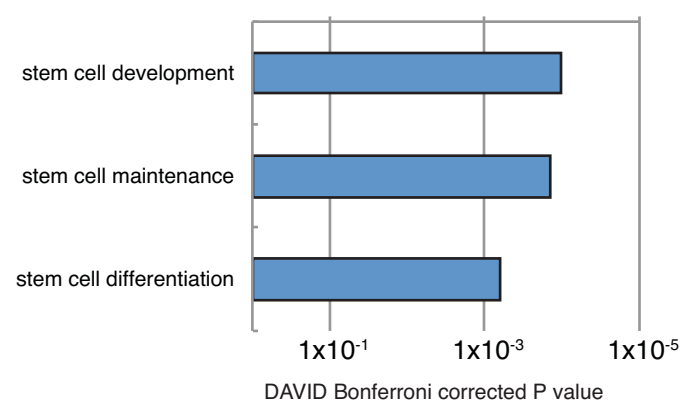

Figure S2

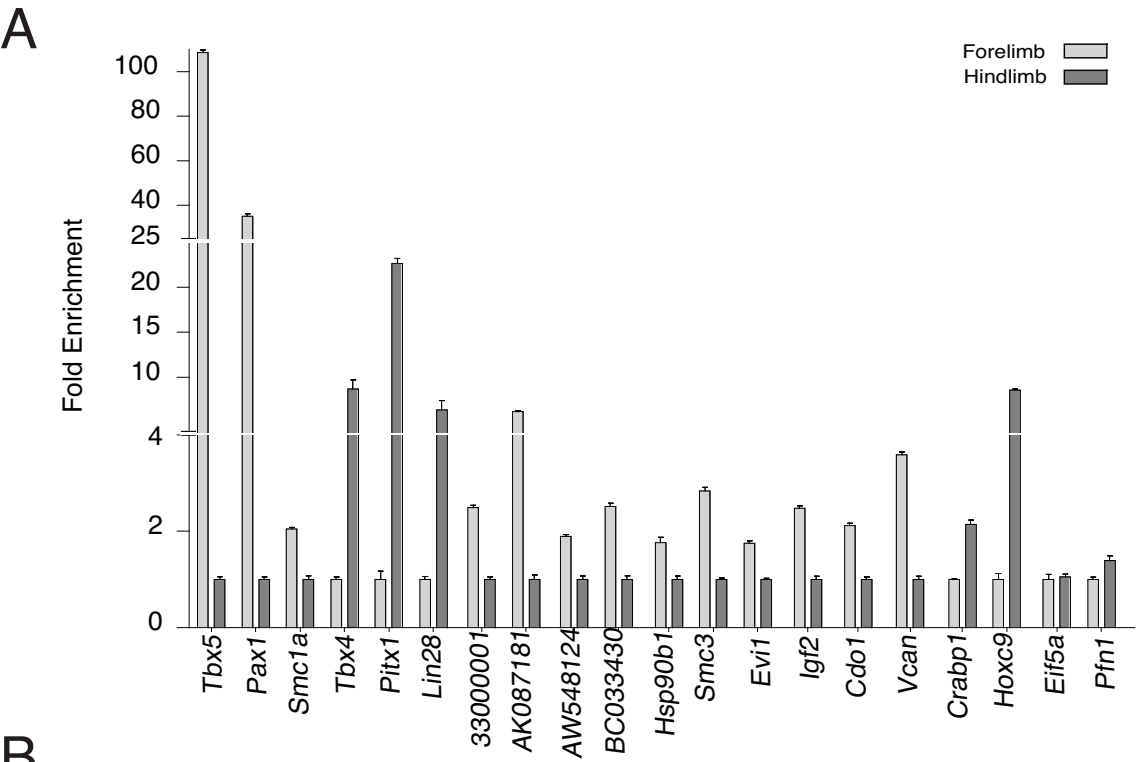
A
Forelimb
Hindlimb
Fold Enrichment
100
80
60
40
25
20
15
10
4
2
0
Tbx5
Pax1
Smc1a
Tbx4
Pitx1
Lin28
33000001
AK087181
AW548124
BC033430
Hsp90b1
Smc3
Evi1
Igf2
Cdo1
Vcan
Crabp1
Hoxc9
Eif5a
Pfn1

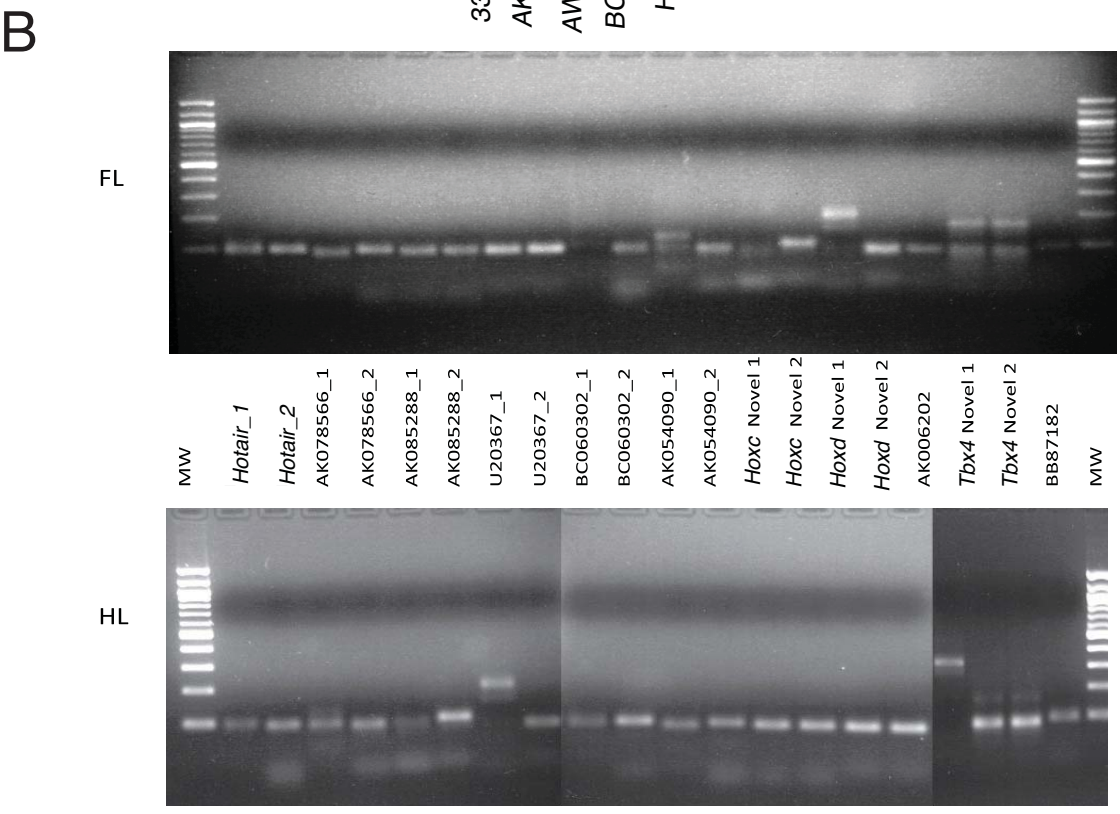
B
FL
HL
MW
Hotair_1
Hotair_2
AK078566_1
AK078566_2
AK085288_1
AK085288_2
U20367_1
U20367_2
BC060302_1
BC060302_2
AK054090_1
AK054090_2
Hoxc Novel 1
Hoxc Novel 2
Hoxd Novel 1
Hoxd Novel 2
AK006202
Tbx4 Novel 1
Tbx4 Novel 2
BB87182
MW

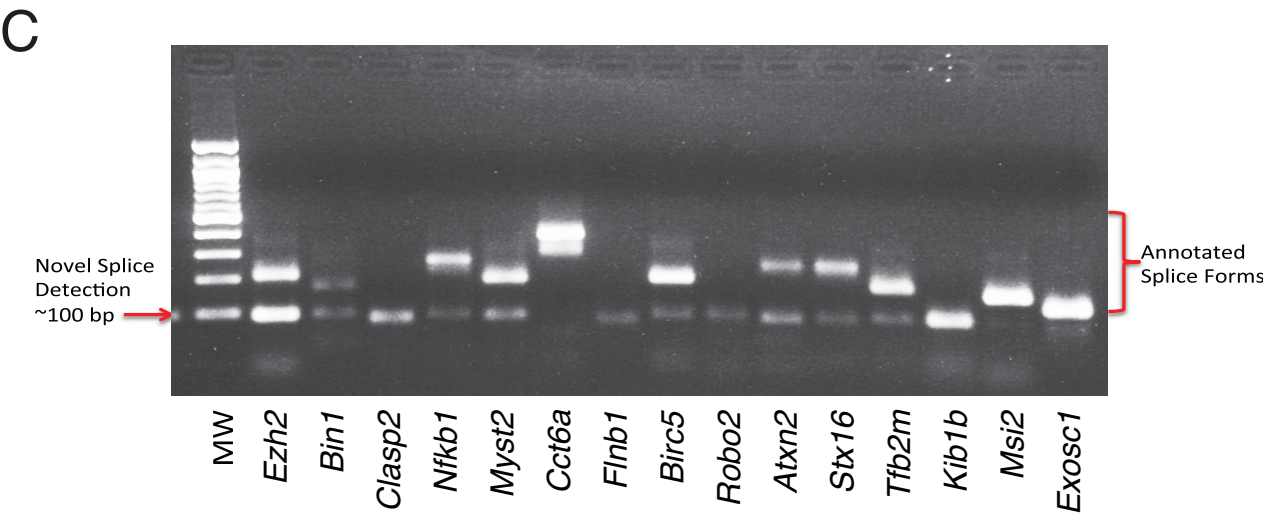
C
Novel Splice
Detection
~100 bp
Annotated
Splice Forms
MW
Ezh2
Bin1
Clasp2
Nfkb1
Myst2
Cct6a
Flnb1
Birc5
Robo2
Atxn2
Stx16
Tfb2m
Kib1b
Msi2
Exosc1

Figure S3

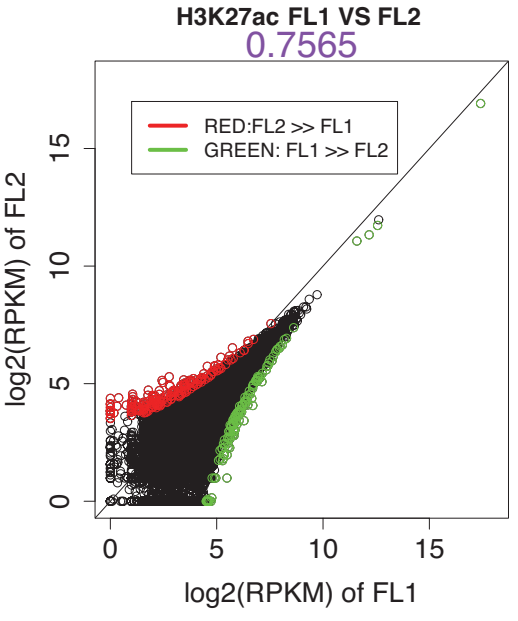
H3K27ac FL1 VS FL2
0.7565
RED:FL2 >> FL1
GREEN: FL1 >> FL2
log2(RPKM) of FL2
log2(RPKM) of FL1
0
5
10
15

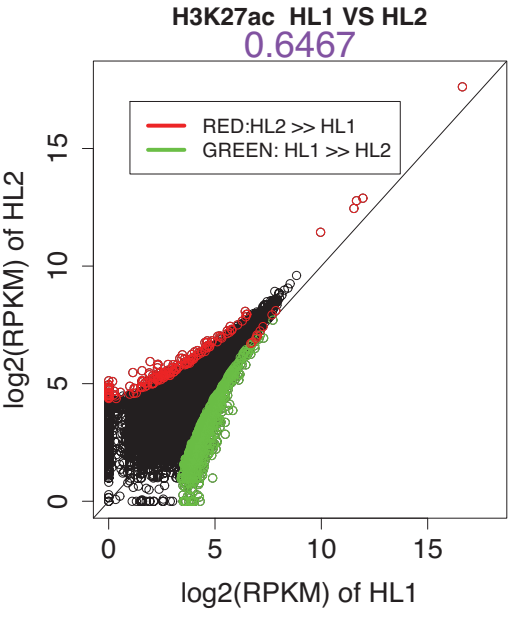
H3K27ac HL1 VS HL2
0.6467
RED:HL2 >> HL1
GREEN: HL1 >> HL2
log2(RPKM) of HL2
log2(RPKM) of HL1
0
5
10
15

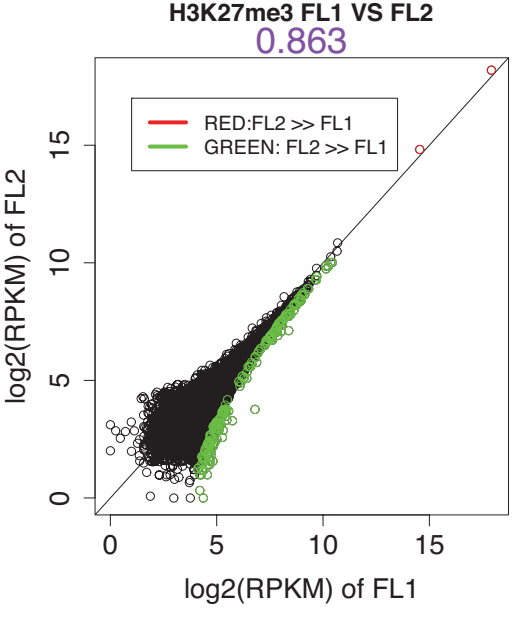
H3K27me3 FL1 VS FL2
0.863
RED:FL2 >> FL1
GREEN: FL2 >> FL1
log2(RPKM) of FL2
log2(RPKM) of FL1
0
5
10
15

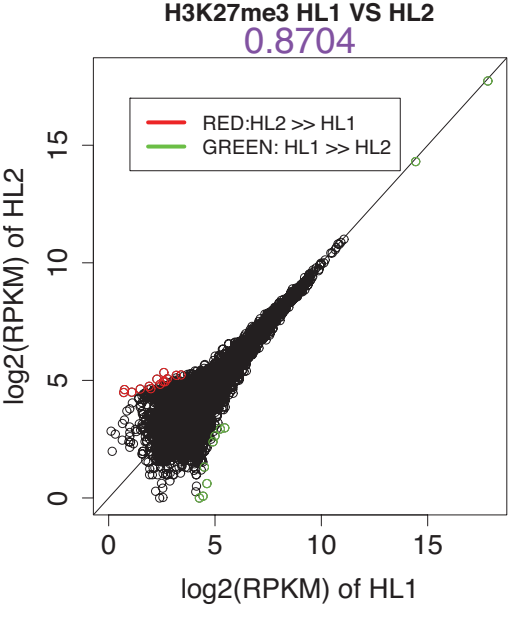
H3K27me3 HL1 VS HL2
0.8704
RED:HL2 >> HL1
GREEN: HL1 >> HL2
log2(RPKM) of HL2
log2(RPKM) of HL1
0
5
10
15

Figure S4

A

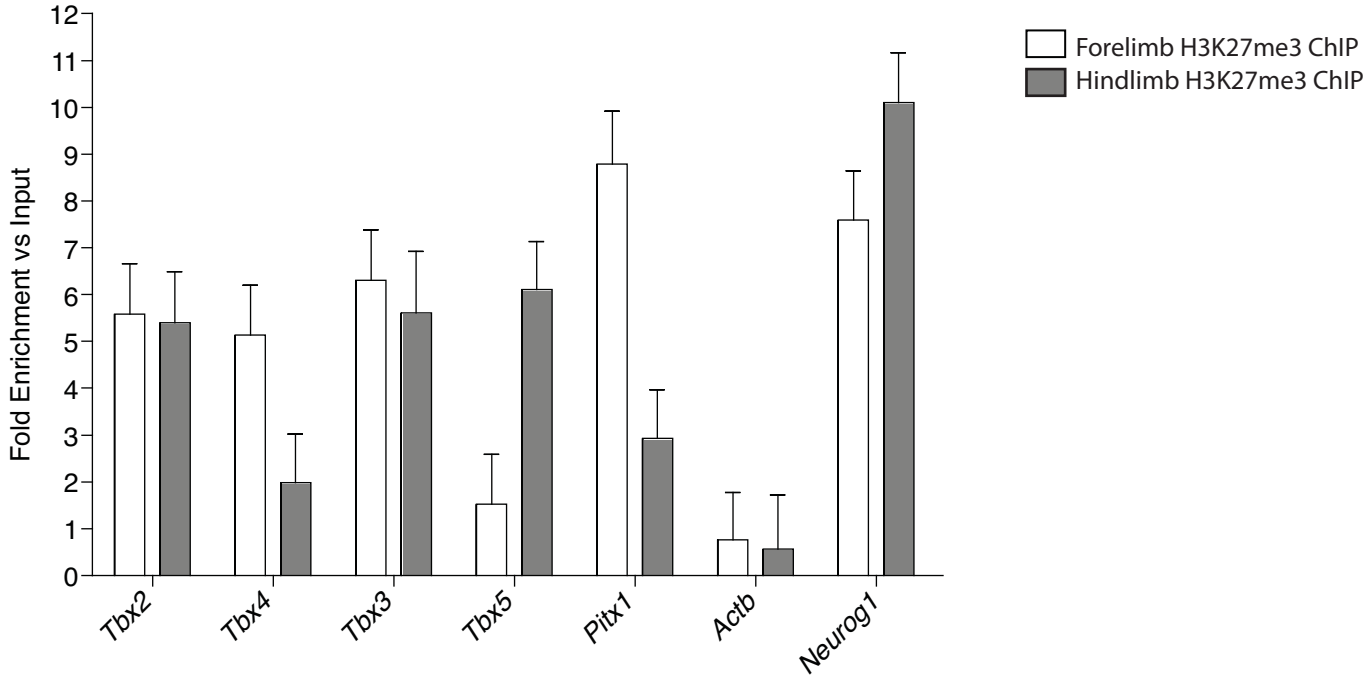
Fold Enrichment vs Input
0
1
2
3
4
5
6
7
8
9
10
11
12
Tbx2
Tbx4
Tbx3
Tbx5
Pitx1
Actb
Neurog1
Forelimb H3K27me3 ChIP
Hindlimb H3K27me3 ChIP

B

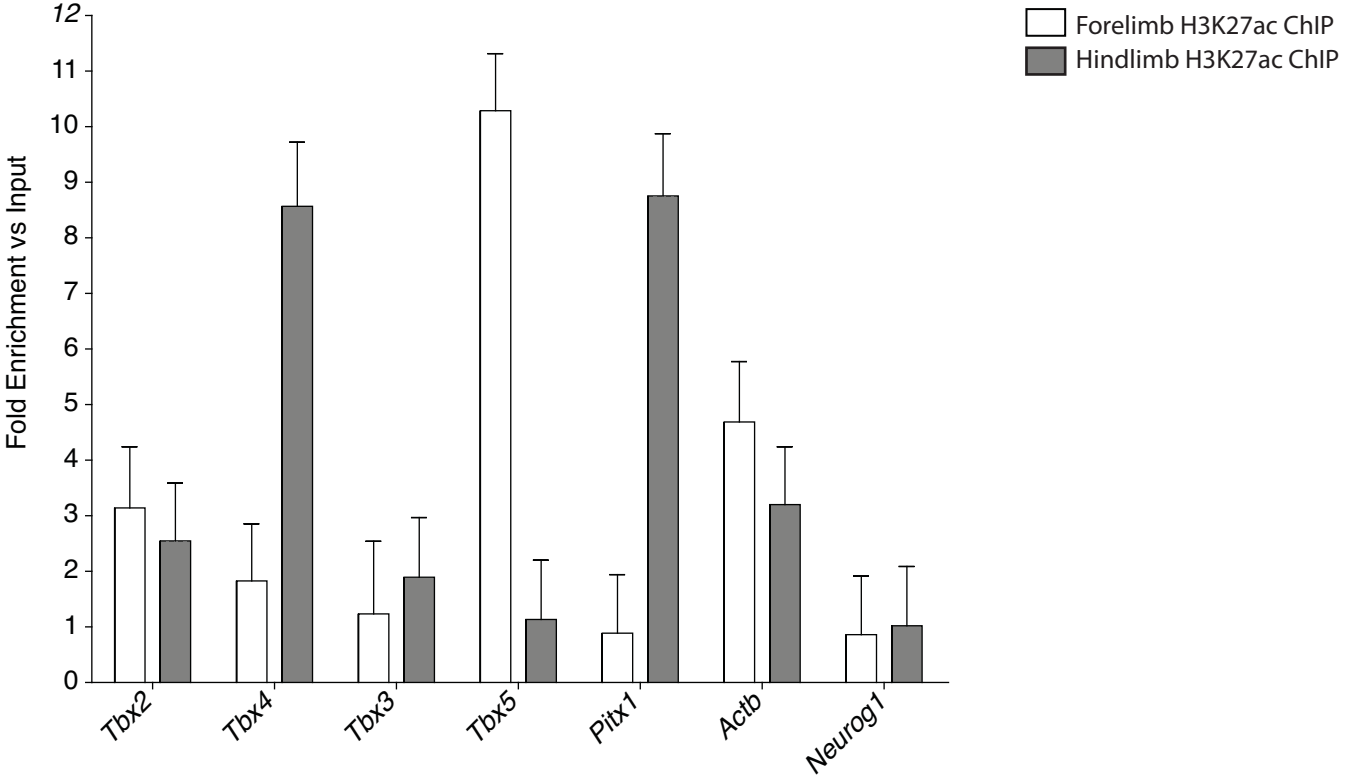
Fold Enrichment vs Input
0
1
2
3
4
5
6
7
8
9
10
11
12
Tbx2
Tbx4
Tbx3
Tbx5
Pitx1
Actb
Neurog1
Forelimb H3K27ac ChIP
Hindlimb H3K27ac ChIP

Figure S5

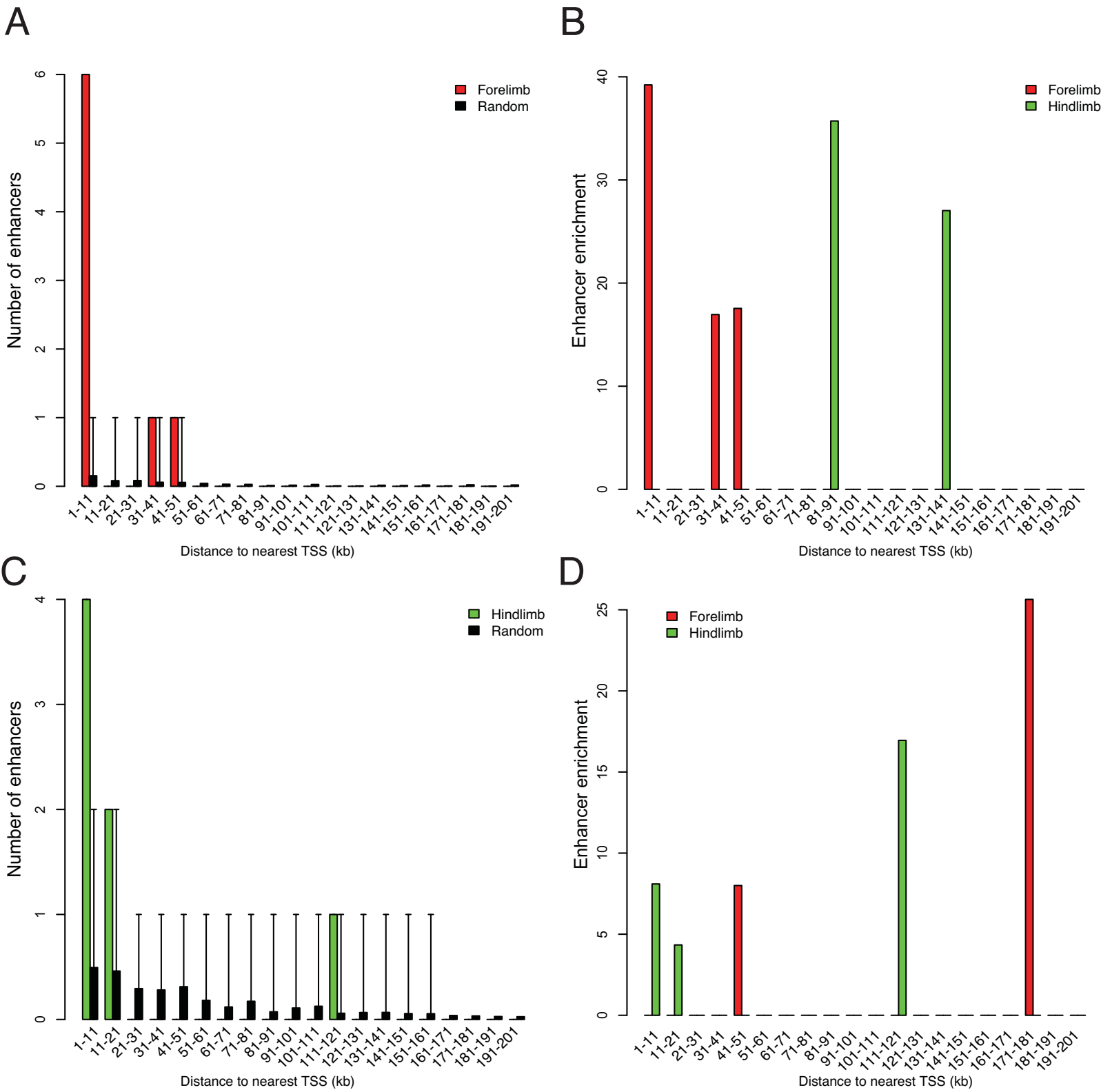
A
Forelimb
Random
Number of enhancers
0
1
2
3
4
5
6
1-11
11-21
21-31
31-41
41-51
51-61
61-71
71-81
81-91
91-101
101-111
111-121
121-131
131-141
141-151
151-161
161-171
171-181
181-191
191-201
Distance to nearest TSS (kb)
B
Forelimb
Hindlimb
Enhancer enrichment
0
10
20
30
40
1-11
11-21
21-31
31-41
41-51
51-61
61-71
71-81
81-91
91-101
101-111
111-121
121-131
131-141
141-151
151-161
161-171
171-181
181-191
191-201
Distance to nearest TSS (kb)
C
Hindlimb
Random
Number of enhancers
0
1
2
3
4
1-11
11-21
21-31
31-41
41-51
51-61
61-71
71-81
81-91
91-101
101-111
111-121
121-131
131-141
141-151
151-161
161-171
171-181
181-191
191-201
Distance to nearest TSS (kb)
D
Forelimb
Hindlimb
Enhancer enrichment
0
5
10
15
20
25
1-11
11-21
21-31
31-41
41-51
51-61
61-71
71-81
81-91
91-101
101-111
111-121
121-131
131-141
141-151
151-161
161-171
171-181
181-191
191-201
Distance to nearest TSS (kb)

Figure S6

A

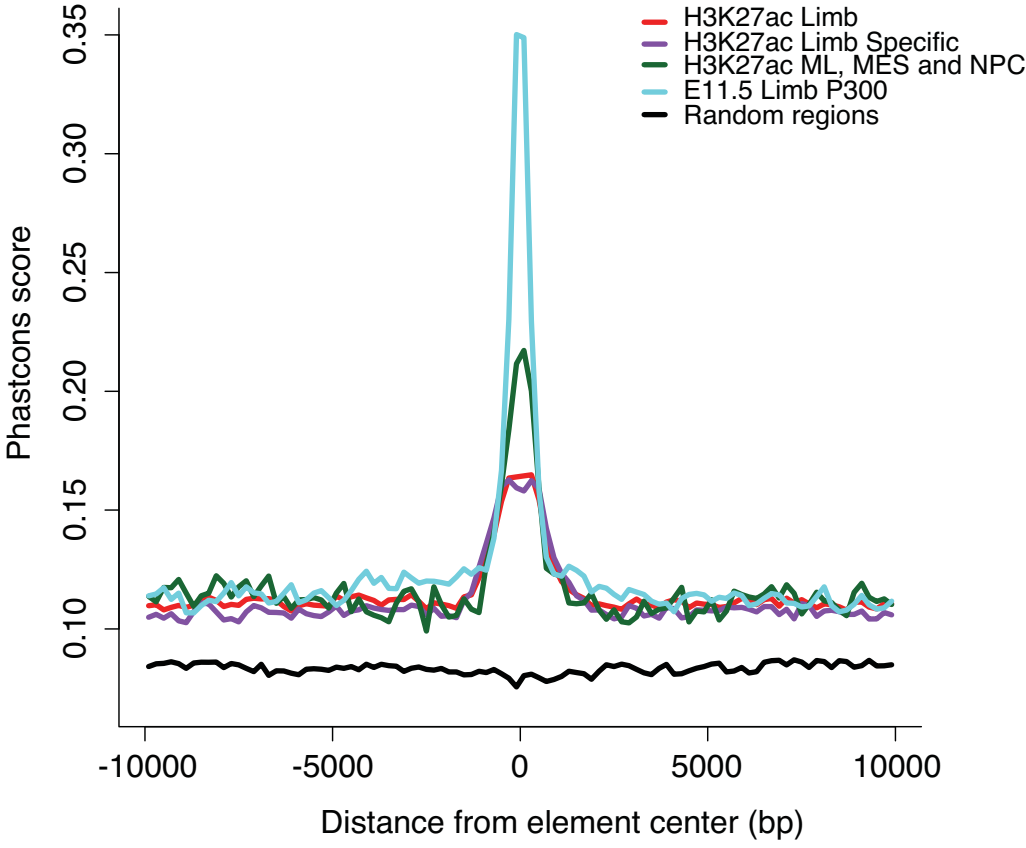
H3K27ac Limb
H3K27ac Limb Specific
H3K27ac ML, MES and NPC
E11.5 Limb P300
Random regions
Phastcons score
0.10
0.15
0.20
0.25
0.30
0.35
-10000
-5000
0
5000
10000
Distance from element center (bp)

Figure S7

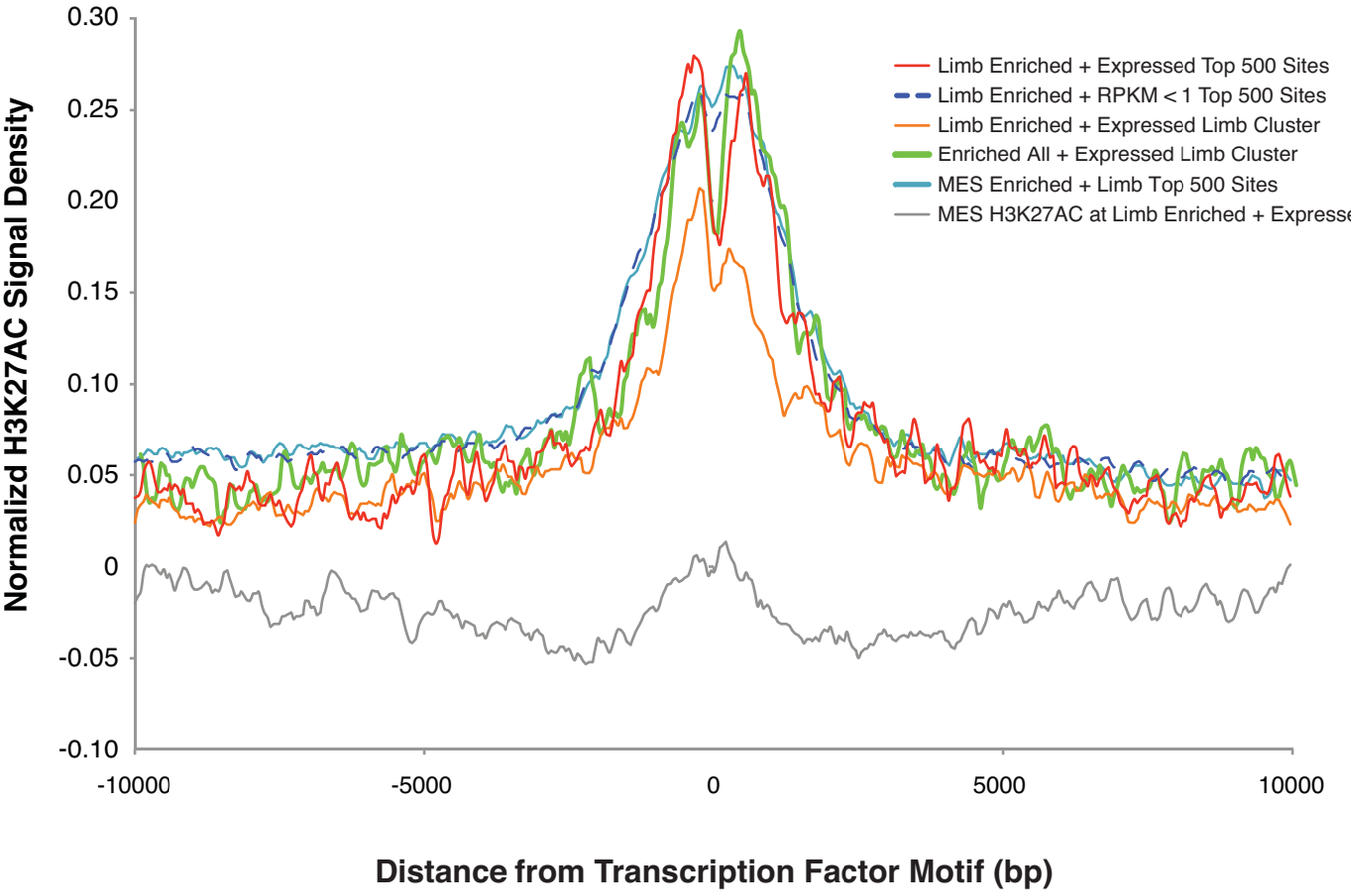
Normalizd H3K27AC Signal Density
0.30
0.25
0.20
0.15
0.10
0.05
0
-0.05
-0.10
-10000
-5000
0
5000
10000
Distance from Transcription Factor Motif (bp)
Limb Enriched + Expressed Top 500 Sites
Limb Enriched + RPKM < 1 Top 500 Sites
Limb Enriched + Expressed Limb Cluster
Enriched All + Expressed Limb Cluster
MES Enriched + Limb Top 500 Sites
MES H3K27AC at Limb Enriched + Expressed

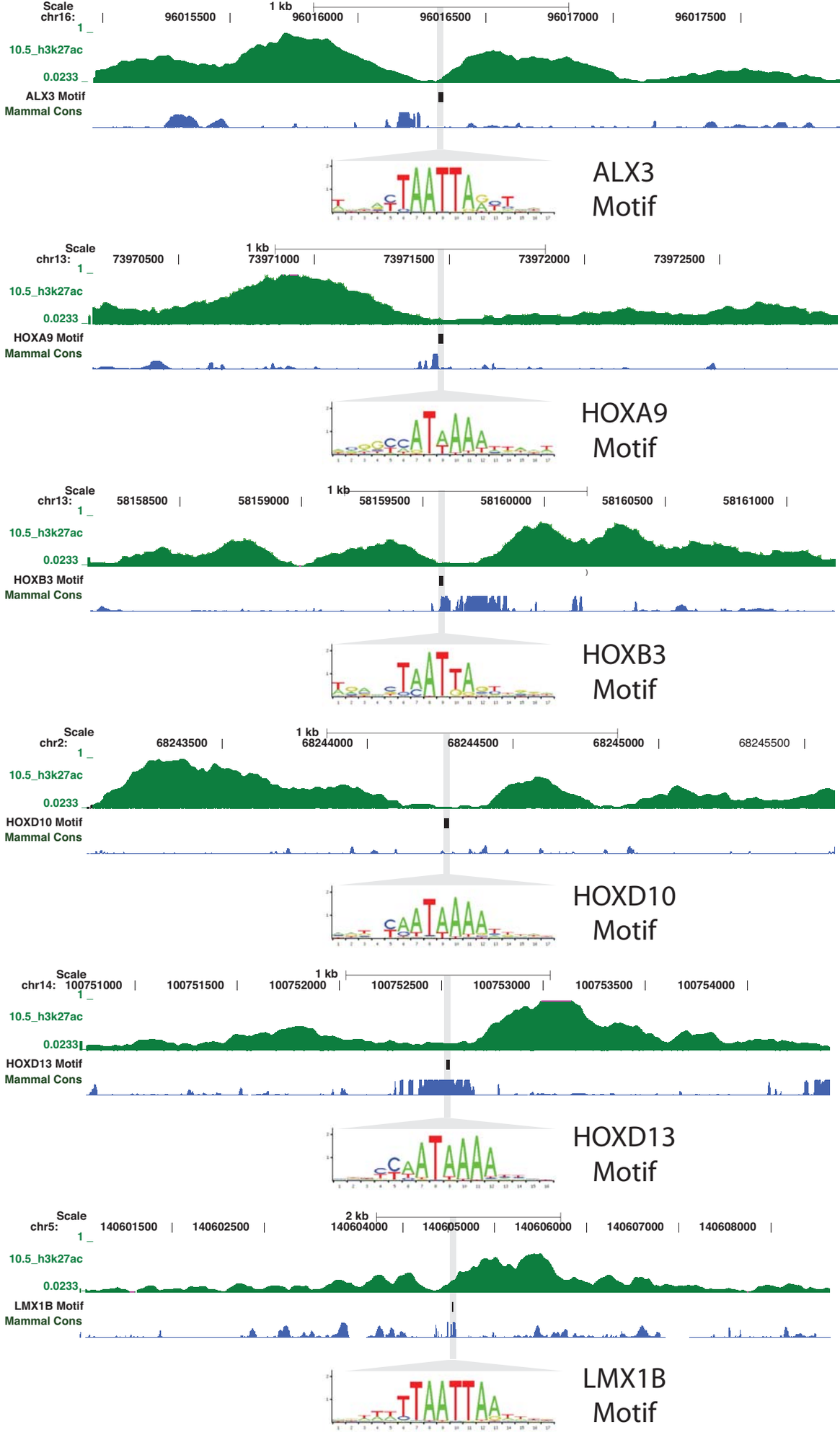
Scale
chr16:
1 kb
96015500
96016000
96016500
96017000
96017500
10.5_h3k27ac
0.0233
ALX3 Motif
Mammal Cons
ALX3 Motif
Scale
chr13:
1 kb
73970500
73971000
73971500
73972000
73972500
10.5_h3k27ac
0.0233
HOXA9 Motif
Mammal Cons
HOXA9 Motif
Scale
chr13:
1 kb
58158500
58159000
58159500
58160000
58160500
58161000
10.5_h3k27ac
0.0233
HOXB3 Motif
Mammal Cons
HOXB3 Motif
Scale
chr2:
1 kb
68243500
68244000
68244500
68245000
68245500
10.5_h3k27ac
0.0233
HOXD10 Motif
Mammal Cons
HOXD10 Motif
Scale
chr14:
1 kb
100751000
100751500
100752000
100752500
100753000
100753500
100754000
10.5_h3k27ac
0.0233
HOXD13 Motif
Mammal Cons
HOXD13 Motif
Scale
chr5:
2 kb
140601500
140602500
140604000
140605000
140606000
140607000
140608000
10.5_h3k27ac
0.0233
LMX1B Motif
Mammal Cons
LMX1B Motif

Figure S8

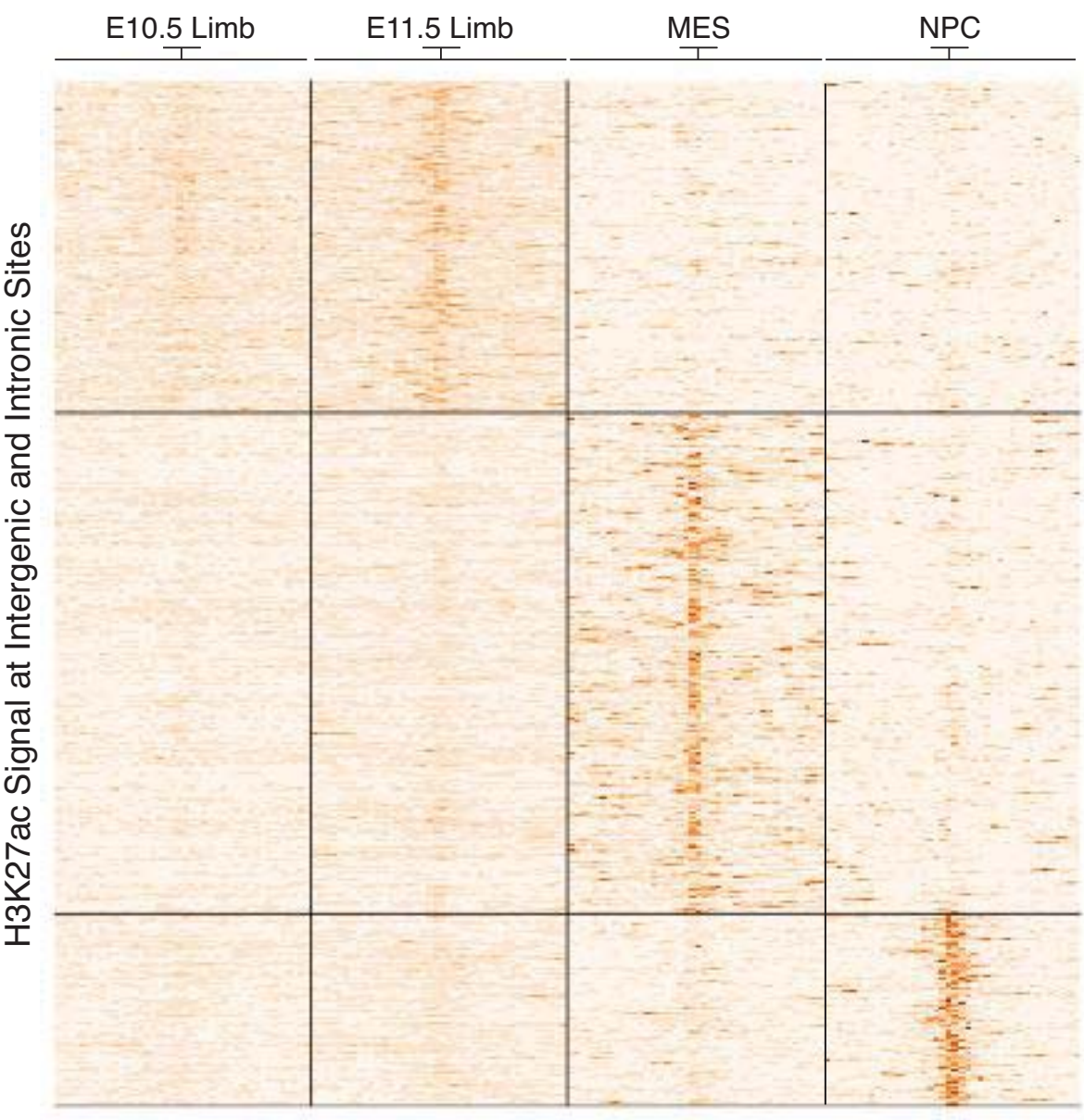
E10.5 Limb
E11.5 Limb
MES
NPC
H3K27ac Signal at Intergenic and Intronic Sites

Figure S9

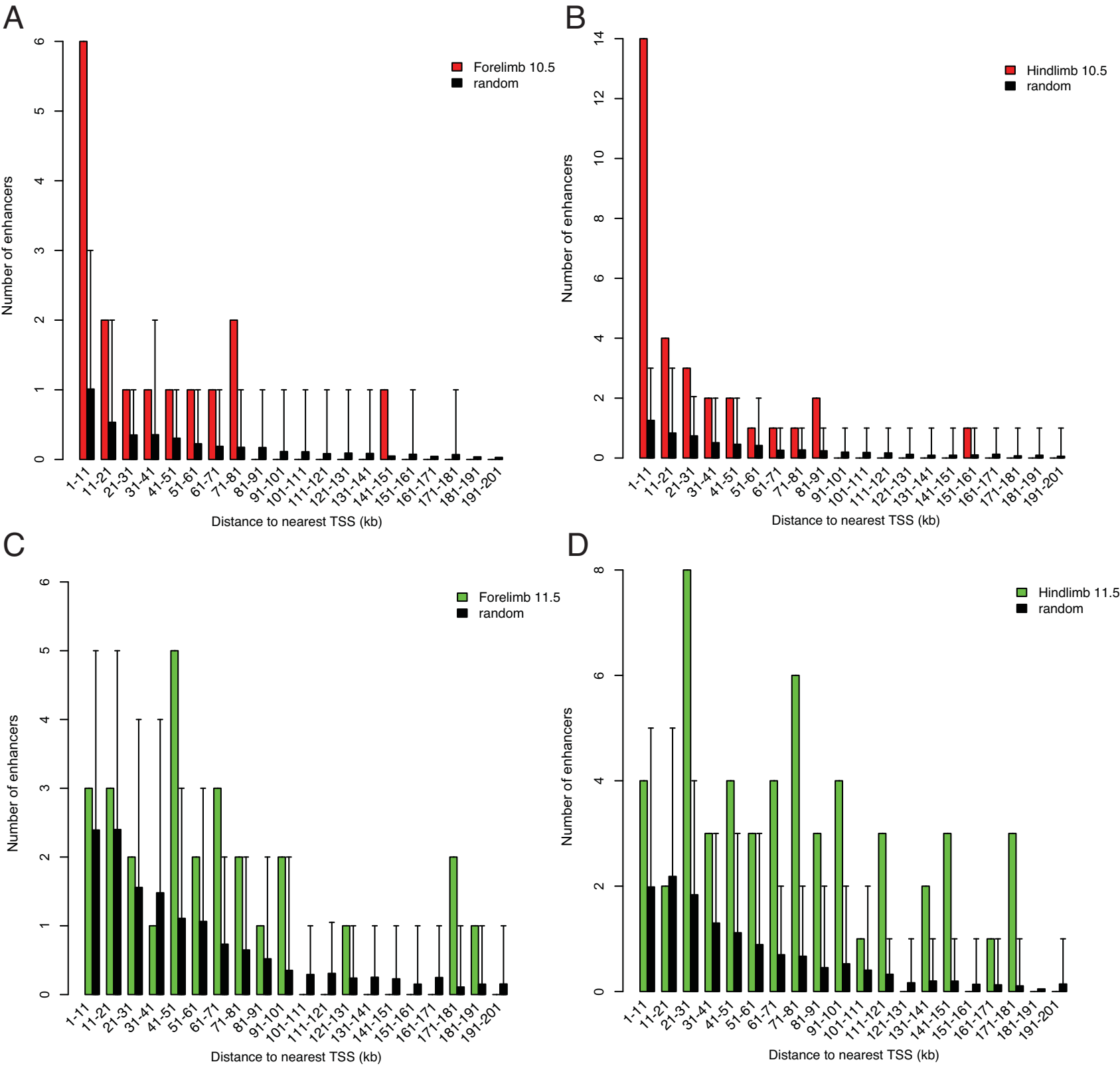
A
Forelimb 10.5
random
Number of enhancers
Distance to nearest TSS (kb)
B
Hindlimb 10.5
random
Number of enhancers
Distance to nearest TSS (kb)
C
Forelimb 11.5
random
Number of enhancers
Distance to nearest TSS (kb)
D
Hindlimb 11.5
random
Number of enhancers
Distance to nearest TSS (kb)
1-11
11-21
21-31
31-41
41-51
51-61
61-71
71-81
81-91
91-101
101-111
111-121
121-131
131-141
141-151
151-161
161-171
171-181
181-191
191-201

Figure S10

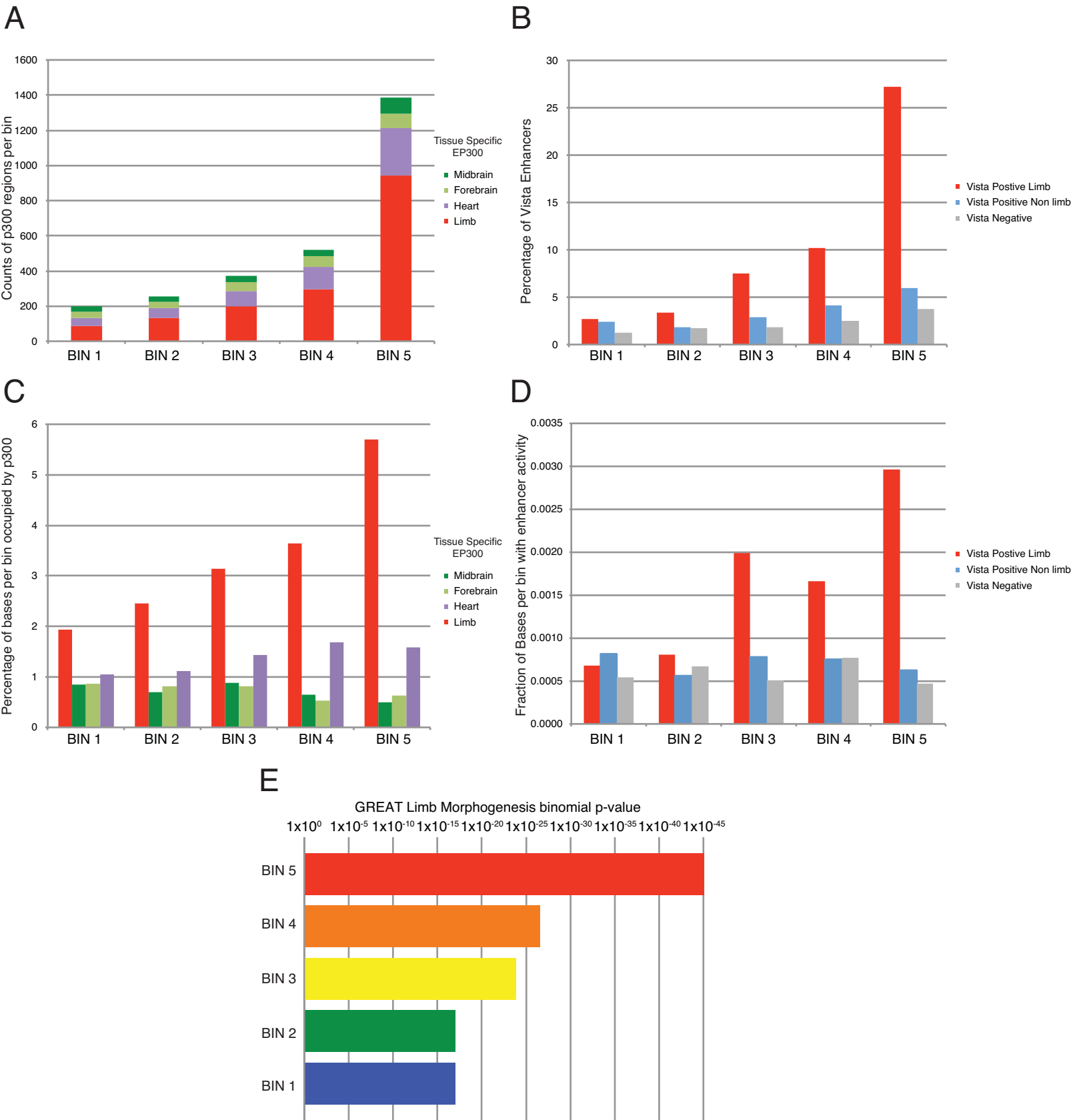
A
Counts of p300 regions per bin
1600
1400
1200
1000
800
600
400
200
0
BIN 1
BIN 2
BIN 3
BIN 4
BIN 5
Tissue Specific EP300
Midbrain
Forebrain
Heart
Limb
B
Percentage of Vista Enhancers
30
25
20
15
10
5
0
BIN 1
BIN 2
BIN 3
BIN 4
BIN 5
Vista Postive Limb
Vista Positive Non limb
Vista Negative
C
Percentage of bases per bin occupied by p300
6
5
4
3
2
1
0
BIN 1
BIN 2
BIN 3
BIN 4
BIN 5
Tissue Specific EP300
Midbrain
Forebrain
Heart
Limb
D
Fraction of Bases per bin with enhancer activity
0.0035
0.0030
0.0025
0.0020
0.0015
0.0010
0.0005
0.0000
BIN 1
BIN 2
BIN 3
BIN 4
BIN 5
Vista Postive Limb
Vista Positive Non limb
Vista Negative
E
GREAT Limb Morphogenesis binomial p-value
1x10^0 1x10^-5 1x10^-10 1x10^-15 1x10^-20 1x10^-25 1x10^-30 1x10^-35 1x10^-40 1x10^-45
BIN 5
BIN 4
BIN 3
BIN 2
BIN 1

Figure S11

A

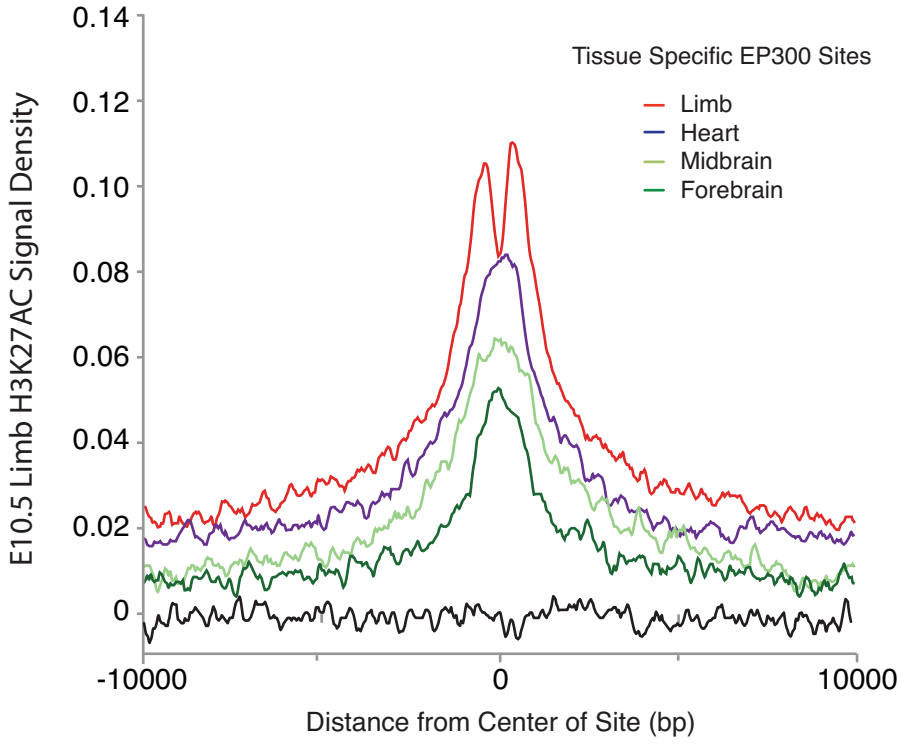

B

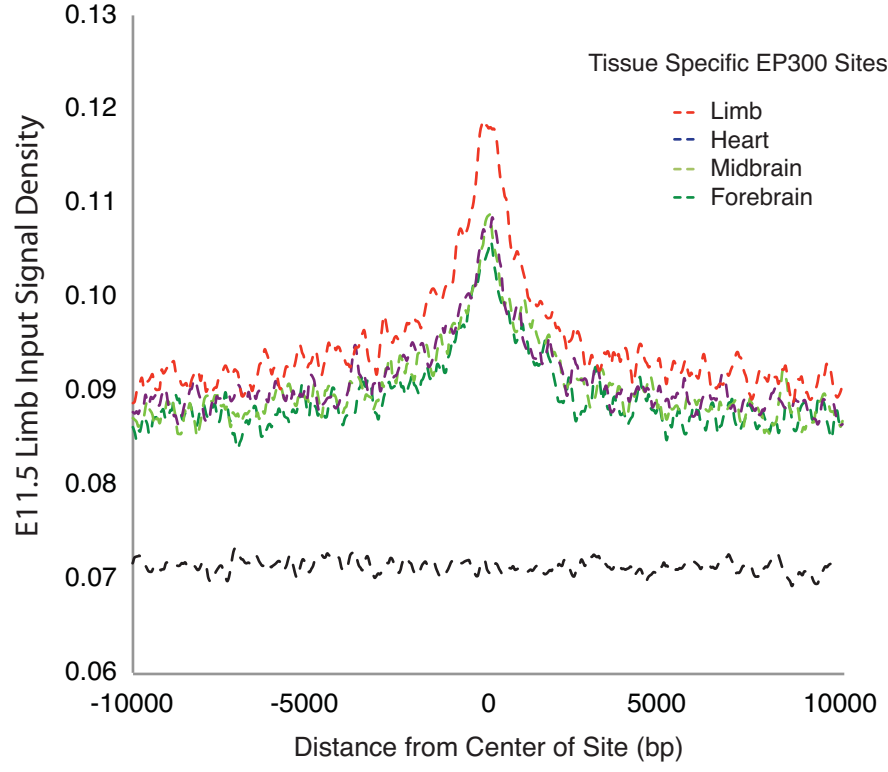

C

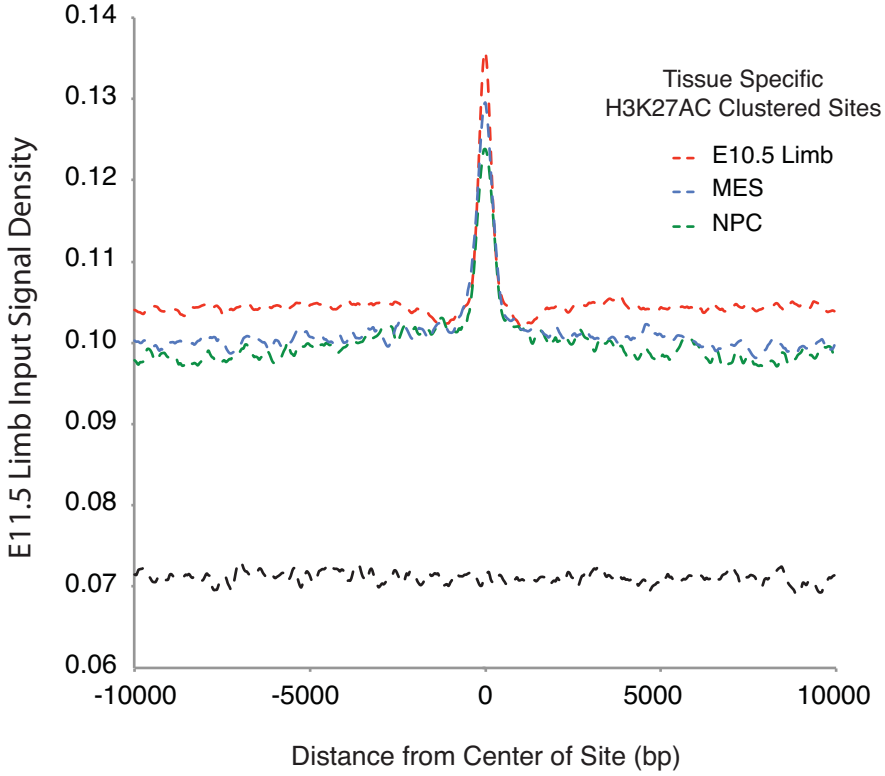

D

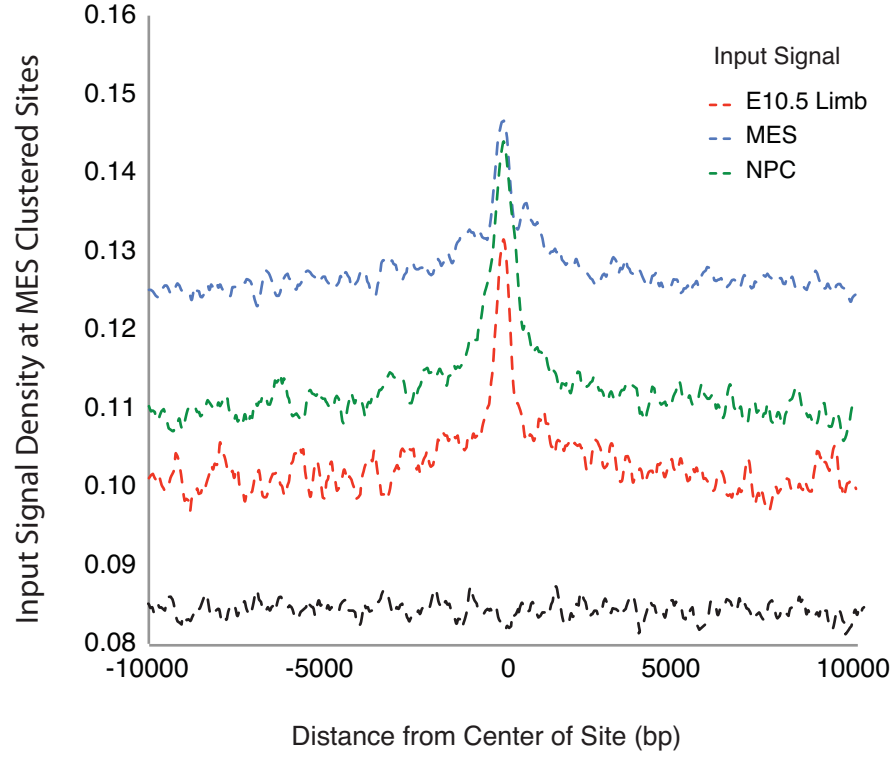

Figure S12

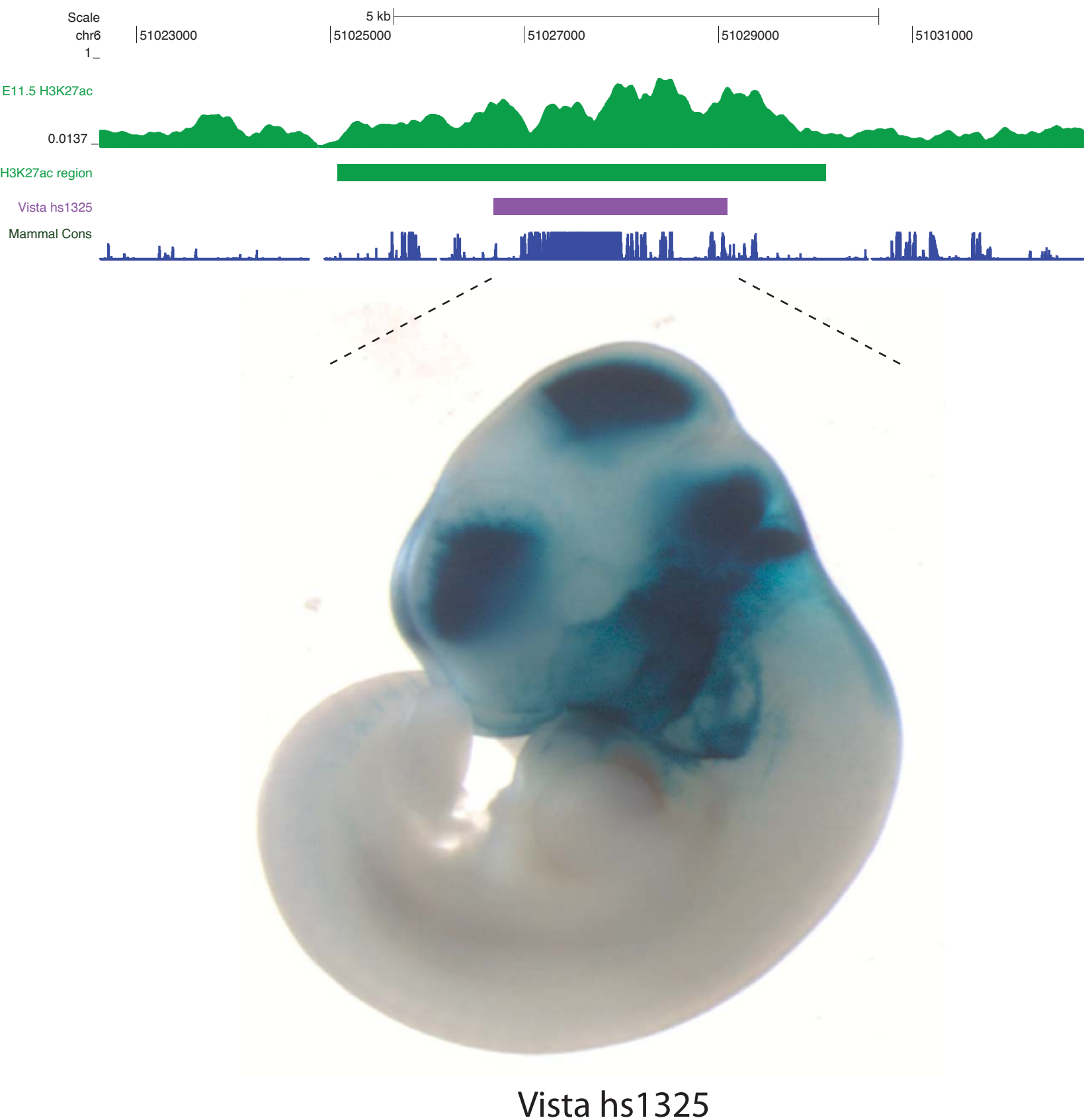
Scale
chr6
1
5 kb
51023000
51025000
51027000
51029000
51031000
E11.5 H3K27ac
0.0137
H3K27ac region
Vista hs1325
Mammal Cons
Vista hs1325